Chapter 4
A GIS for Flood Risk Management in Flanders

Pieter Deckers, Wim Kellens, Johan Reyns, Wouter Vanneuville, and Philippe De Maeyer

Abstract In the past decades, Flanders, a region of north Belgium that extends from the coastline inland (in northwest Europe), has suffered several serious riverine floods that caused substantial property damage. As Flanders is one of the most densely populated regions in the world, a solid water management policy is needed in order to mitigate the effects of this type of calamity. In the past, Flemish water managers chose to drain off river water as quickly as possible by heightening the dikes along the rivers. However, this method leads to a higher flood probability further downstream. Moreover, water defence infrastructure can always suffer from technical failures (e.g., breaching) creating even more damage than would have occurred if no defences were in place. In a search for a better solution to this recurring problem, the Flemish administration proposed a new approach in the 1990s. This approach focuses on minimizing the consequences of flooding instead of attempting to prevent floods. To implement this approach, large amounts of data were gathered for the Flemish Region. Using a Geographic Information System (GIS), a risk-based methodology was created to quantitatively assess flood risk based on hydrologic models, land use information and socio-economic data. Recently, this methodology was implemented in a specifically designed GIS-based flood risk assessment tool called *LATIS*. By estimating the potential damage and number of casualties during a flood event, *LATIS* offers the possibility to perform risk analysis quickly and effectively. This chapter presents a concise overview of *LATIS*' methodology and its implementation for flood risk management in Flanders.

Keywords Floods · Damage · Risk · Flanders · GIS · Modeling

P. Deckers (✉)
Department of Geography, Faculty of Sciences, Ghent University,
Krijgslaan 281, 9000 Gent, Belgium
e-mail: pieter.deckers@ugent.be

P.S. Showalter, Y. Lu (eds.), *Geospatial Techniques in Urban Hazard and Disaster Analysis*,
Geotechnologies and the Environment 2, DOI 10.1007/978-90-481-2238-7_4,

4.1 Introduction

Flanders is located in the centre of northwest Europe, in the low-lying northern part of Belgium, bordering the North Sea (Fig. 4.1). The region is characterised by a number of river valleys with moderate slopes and minor elevation differences. During heavy torrents or long-lasting rainy weather, parts of Flanders are regularly flooded due to overflow (and in rare occasions by breaching) of river dikes. For example, the Dender catchment (the dark grey region west of Brussels indicated by the "D" in Fig. 4.1) suffered heavy floods in 1995, 1999 and 2002–2003.

As Flanders is one of the most densely populated and industrialised regions in the world, adequate flood risk management is necessary. In the past, the solution of the Flemish administration to the flood problem was to drain the water downstream as quickly as possible by heightening the dikes along the river banks. However, experience showed that this was far from an ideal solution. It has become clear that this method leads to higher water levels and a higher flood risk downstream. Moreover, water defence infrastructure can collapse due to technical failure such as breaching, often creating more damage than would have occurred if no flood defence infrastructure had existed.

The Flemish minister responsible for addressing these types of issues launched a new approach in the governmental note, "Mobility and Public Works 2000−2004" (Vanneuville et al. 2003). The new idea was a paradigm shift away from attempting to protect against high water levels to reducing damages caused by the water. This

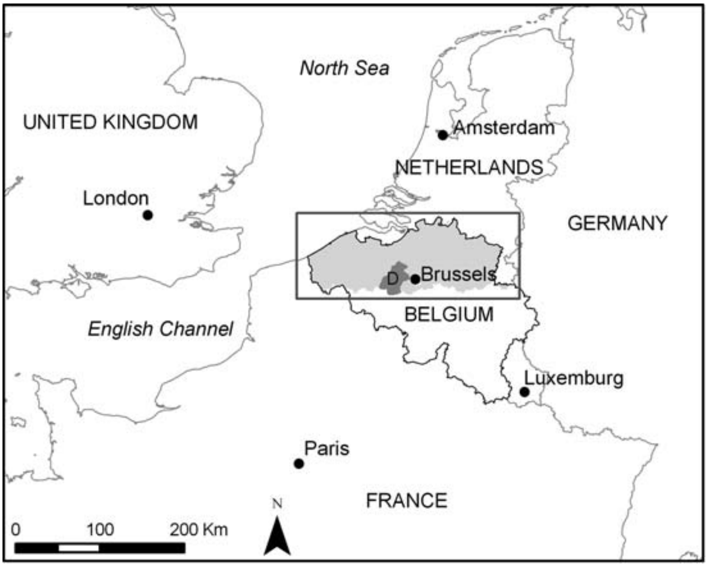

Fig. 4.1 Situation of the region of Flanders (the *gray* region in the *rectangle*) in northwest Europe Source: Vector versie van het "Voorlopig Referentiebestand Gemeentegrenzen", AGIV, toestand 22/05/2003 (GIS-Vlaanderen) and – Vectoriële versie van de "VHA-waterlopen and –zones", Vlaamse Milieumaatschappij – Afdeling Operationeel Waterbeheer (AGIV)

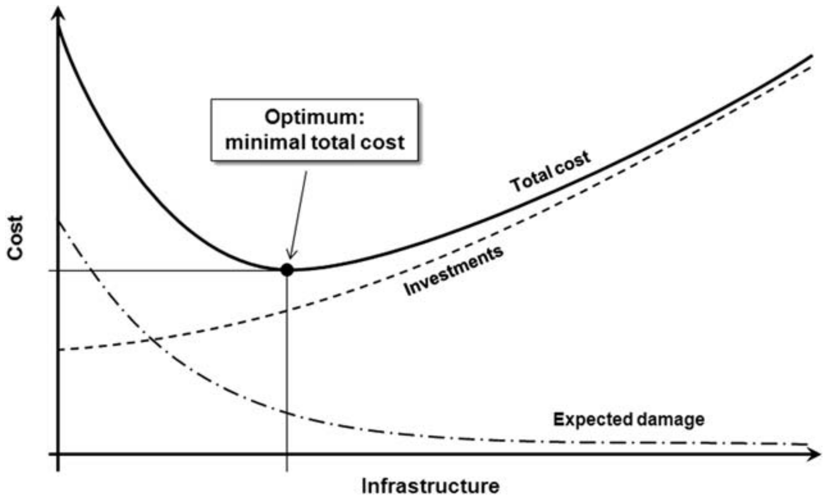

Fig. 4.2 Economic optimum in a cost benefit analysis for water infrastructure

shift created the need to identify the level of investment represented on the landscape (e.g., buildings, infrastructure) and the cost of repairing those investments following a flood. Figure 4.2 provides a graph of this cost benefit analysis, where a point has been placed on the "Total cost" to illustrate the "Optimum minimal total cost". The lower the investment in flood defence infrastructure, the higher the expected costs for damage. As investments in infrastructure increase, expected damage decreases as does the total cost. At a certain point, higher investments no longer lead to major decreases in expected damages and the total cost begins to increase again. At this point, the total cost of investments and expected damage is minimal (De Nocker et al. 2004).

In agricultural areas, the impacts of floods are limited due to low population density, fewer buildings, and reduced amounts of infrastructure. In other areas (e.g., nature conservation zones), flooding can even have positive effects. The opposite is true in densely populated areas or in areas with important industrial activities. In these areas, extra effort and investment must be made to try to reduce the effects of flooding, such as delineating controlled inundation areas to provide short term storage for large volumes of water. In order to estimate and compare the benefits from each of different types of measures, a uniform risk analysis approach is necessary. In this context, several objectives were set by policy makers in the governmental note described earlier (Vanneuville et al. 2003):

- The development of a methodology for the uniform calculation of damage and risk for the whole of Flanders;
- Use of this methodology to calculate change in flood risk and damage due to change in local infrastructure works and/or land use; and,
- A definition of data and software necessary for running the equations in a geographic information technology (GIT) environment.

To meet these goals, Flanders Hydraulics Research,[1] in cooperation with the Department of Geography at Ghent University, developed a risk-based methodology to assess potential flood damage. This chapter describes how the risk-based methodology was implemented via the assessment tool *LATIS*, providing an overview of the input data, chosen assumptions, and different calculations performed. The methodological framework is provided, as well as how flow velocity was modeled as a damage factor and how flood casualties are calculated. Because there is a need for more effective and adaptable tools, *LATIS* is offered as a substitute for earlier GIS-based models. The capability of using *LATIS* to calculate flood risk scenarios with regard to climate change is also demonstrated. The chapter concludes by discussing methodological issues and future research.

4.2 Overview of the Risk-Based Methodology

Generally, risk is defined by the probability of an event (e.g., a flood) and the magnitude of its consequences (Jacobs and Worthley 1999). These consequences can be measured in terms such as buildings damaged or lives lost (Ahola et al. 2007). Although some researchers have added additional criteria to the definition of risk, flood risk studies in European countries are usually performed using the combination of probability and consequences (Verwaest et al. 2008). The methodology described in this chapter follows this general definition.

Several steps are required to calculate damage and risk (Vanneuville et al. 2005), as is shown in Fig. 4.3. The first step requires the generation of a set of flood maps, each representing the extent of a flood with a certain return period, using hydrological, hydraulic, and digital elevation models. Second, different land use maps are combined with a variety of socio-economic data resulting in a maximum damage map. This maximum damage map is subsequently combined with the different flood maps to create damage maps for each return period. In the final phase, these damage maps are combined into a single risk map.

4.2.1 Flood Map Calculations

Before calculating damage and risk, it is necessary to estimate an area's flooding probability through statistical analysis of past water levels and flow rates. First, the return period, or average period of time in which a particular maximum water level and discharge may occur, is calculated. Higher water levels and discharge volumes correspond to longer return periods of occurrence. Calculating probability of occurrence is performed using composite hydrographs, which are synthetic hydrographs integrated from Quantity/Duration/Frequency (QDF)-relationships. These

[1] Flanders Hydraulics Research is part of the Department of Mobility and Public Works of the Flemish Government and is responsible for the navigable waterways in Flanders.

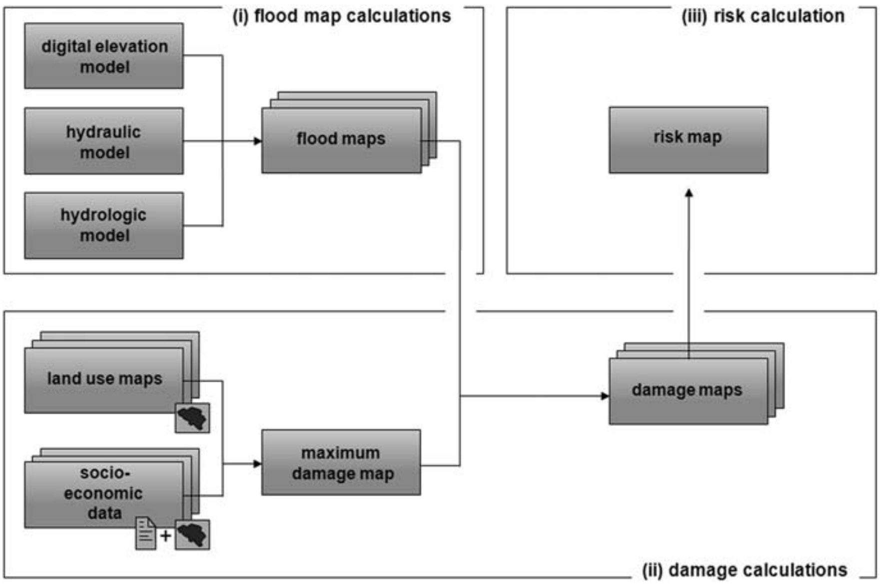

Fig. 4.3 Framework for risk mapping (to be read counterclockwise, starting at *upper left*)

QDF-relationships statistically link every river discharge with its duration and return period. Composite hydrographs have the advantage that in every point along the waterway (and in the flood zones) the calculated water levels have the same return period. Only one calculation is required for every return period, resulting in more rapid risk calculation models (Vaes et al. 2002).

As stated above, flood maps are created using hydrological, hydraulic, and digital elevation models. These maps show maximum water levels and flooding extent. Additional information such as flow velocity and the "rise velocity" of water (especially important for casualty assessment) can also be obtained. Thus for each return period, a set of maps is available indicating flood extent, flow velocity and rise velocity. Since creating and validating composite hydrographs is time-consuming, only a discrete set of flood maps was created (e.g., 1, 2, 5, 10, 25, 50, 100, 250 years for the Dender catchment). If more historical data are available, flood maps for even longer return periods can be calculated.

4.2.2 Damage Calculations

In this step, land use information and socio-economic data are used to produce a maximum damage map. This maximum damage map contains the potential damage value per surface area, where maximal damage can occur from a hazardous event. Put differently, this map indicates the cost value for a virtual scenario in which everything is destroyed by a (flood) event. By combining the maximum damage map with the flood maps, expected damage for a given inundation can be calculated.

4.2.2.1 Different Types of Damage

Numerous definitions of damage can be found in the disaster literature (e.g., Cochrane 2004). However, a number of distinctions are common with regard to flooding (De Maeyer et al. 2003). Financially, damage can be split into monetary (tangible) and non-monetary (intangible – including emotional) damage. A second classification can be made between internal and external damage. Internal damage is damage caused in the inundated zone itself, external damage occurs outside the inundated area. An example of the latter is production loss due to economic dependence on customers and/or suppliers located in the flooded area. A third classification is between direct and indirect damage. The first refers to damage affecting buildings, furniture, stocks, crops, and the like while the second refers to production losses and clean-up costs.

The risk methodology used here only considers monetary, internal, and direct/indirect damage. Although several authors have performed flood risk assessment including non-monetary (Yates 1992; Lekuthai and Vongvisessomjai 2001; Simonovic and Carson 2003) and external damage (Penning-Rowsell et al. 2003; Van der Veen and Logtmeijer 2005), these criteria were beyond the scope of this study.

4.2.2.2 Maximum Damage Map

Different land use categories have different potential maximum damage values. Damage values for completely destroyed cropland are less when compared to the total destruction of a factory. Therefore, land use information is needed to create a maximum damage map. Two major resources were used to create an overall land use map of Flanders: CORINE Land Cover (a classified land use map that covers all European member states) and the Small Scale Land Use map of Flanders and Brussels.[2] The combination of these data makes it possible to classify land use into different categories such as built-up areas, industrial grounds, crop lands, pastures, transport infrastructure and airports (Vanneuville et al. 2003). Both CORINE Land Cover and the Small Scale Land Use Map are based on LANDSAT images with a resolution of 30 m per pixel. As this resolution was insufficient to fulfill all needs, vector-based land use information such as road and railroad networks, and locations of highly valued buildings (e.g., hospitals, fire stations, schools, churches, electricity and communication infrastructure) was added to the database.

Once land use information is available, the maximum damage values have to be linked to the land use categories. To perform this task, socio-economic data is gathered. As it is difficult[3] to incorporate the individual value of each household, factory

---

[2]Both land use maps are included for two reasons: (i) the combination provides additional land use information unavailable when using only one data source, and (ii) each data set has a different renewal period, so the most recent land use map can be used when required.

[3]Insurance companies possess information on the monetary value of individual households, but are generally unwilling to disclose such private information. For croplands, another problem arises

or cropland, aggregated spatial data was used (e.g., mean housing value per statistical area, average value of crops per agricultural area, average value of factories per industrial sector). This approach causes every house in a particular statistical area to have the identical maximum damage value, but homes in residential areas will have higher values than those found in areas that are economically disadvantaged. Similarly, croplands in agricultural areas where fruits and vegetables are most important will carry a higher maximum damage value than croplands in agricultural areas where potatoes and cereals are more common. Data was gathered and grouped for each land use category (for a detailed description, see Vanneuville et al. 2003). After combining the land use map with the damage values, a maximum damage map can be produced.

4.2.2.3 Calculating Damage Maps

The next step combines the maximum damage map with the different flood maps to create maps of real flood damage suffered during each return period. Floods rarely lead to total destruction. The extent of damage depends on water depth because all land use categories have different relationships between the amount of damage that occurs and water depth. These relationships are defined by damage functions or α-factors (Penning-Rowsell et al. 2003). To illustrate, five different damage functions are shown in Fig. 4.4. The quantitative relationship reflected in these functions

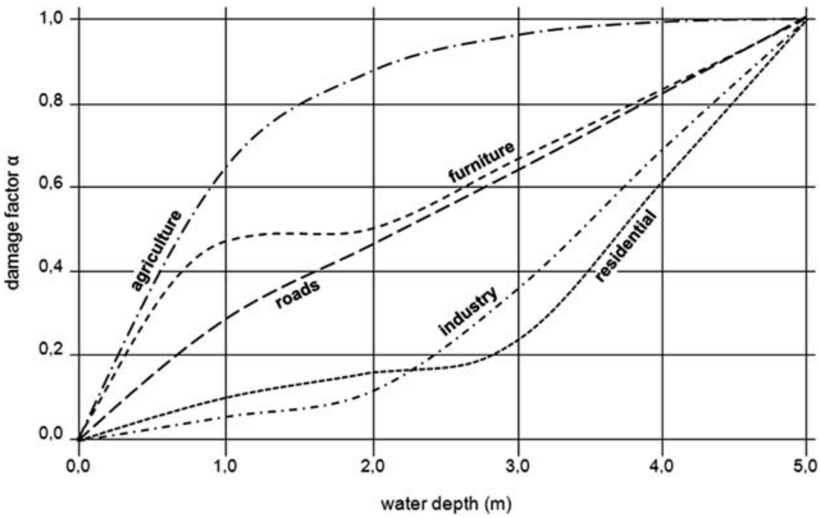

Fig. 4.4 Damage functions: real damage as a function of water depth

because of regular shifts in cultivation. For example, one year potatoes may be cultivated and the next corn; the gathering of such information is very intensive, time-consuming and sometimes impossible (due to privacy reasons).

are based on Van de Sande and Corné (2001) and Vanneuville et al. (2003). Each damage function represents a relationship between a given water depth (X-axis) and the dependent damage factor (Y-axis) that can be expected for that land use category. For example, a water depth of 3 m equals a damage factor of approximately 0.36 (36%) for industry. The same water depth causes nearly 100% damage to agriculture. The odd shape of the furniture curve is caused by the assumption that all homes and offices have a "ground floor" containing furniture and the slightest amount of water depth can cause substantial damage. A water depth of 2 m or higher corresponds to an increasing damage factor caused by the appearance of furniture installed on higher floors of a building.

Another important concept in our approach is the "doorstep level" (Vanneuville et al. 2003), or the height above ground level that defines the "zero" level for damage. For industry and housing the "doorstep level" is a physical reality; the concept is based on calibration methods performed in the Netherlands, by which people were asked to indicate the water height above their doorsteps (Vrisou Van Eck et al. 1999). Water levels were conservatively grouped into 25 cm increments, with all water levels in the flood map rounded to the next multiple of 25 cm. Below the "doorstep level", damage is set to zero. For housing, the doorstep level is 25 cm, whereas for roads and industry the doorstep is 50 cm (for roads, the assumption is that low water heights do not cause any damage in the short term). For all other classes of land use, the doorstep level is 0 cm, meaning that damage occurs the moment there is water.

In a flood zone the real damage caused by inundation at a certain water height can be calculated by summing all unique surface entities (i.e., discrete land use categories) and combining the water depth (translated to the corresponding α-factor, the parameter that is represented in Fig. 4.4) with the maximum damage of that land use category. Mathematically, this is described as:

$$S_w = \sum_{landusei} \alpha_i \times S_{i,\max} \tag{4.1}$$

Where

S_w : real damage in a zone
$S_{i,max}$: maximal damage in a land use class *i*
α_i : coefficient expressing the relationship between water depth and damage for land use class *i*

4.2.3 Risk Calculation

In the final step, the different damage maps for each return period are combined into one risk map. As stated above, risk is defined as the probability of a certain event multiplied by the damage caused by that event. The risk (expressed as the mean annual damage per surface unit per year) is then equal to the damage caused by an event with a 1-year return period, plus half of the damage difference between a 2-year flood and a 1-year flood, plus one-third of the damage difference between a 3-year flood and a 2-year flood, and so forth. The mathematical explanation of this procedure is explained in Equations 4.2 and 4.3:

$$R = \sum_{i=1}^{n} \frac{1}{i}(S_i - S_{i-1}) \tag{4.2}$$

Or

$$R = \frac{1}{1}S_1 + \frac{1}{2}(S_2 - S_1) + \frac{1}{3}(S_3 - S_2) + ... + \frac{1}{n}(S_n - S_{n-1}) \tag{4.3}$$

Where

R risk
S_i the damages related to a flood with a return period of i years
n the highest return period

As explained above, the creation and validation of flood maps is time-consuming, so only a few have been created. To calculate risk in practice, it is assumed that linear interpolation of the flood damage between two return periods is valid, so the formula (in the case of return periods of 1, 2, 5, 10, 25, 50 and 100 years) can be simplified to (Vanneuville et al. 2003):

$$R = \frac{1}{1}S_1 + \frac{1}{2}(S_2 - S_1) + \frac{\frac{1}{3}+\frac{1}{4}+\frac{1}{5}}{5-2}(S_5 - S_2) + \frac{\frac{1}{6}+\frac{1}{7}+\frac{1}{8}+\frac{1}{9}+\frac{1}{10}}{10-5}(S_{10} - S_5) + ... \tag{4.4}$$

Equation 4.4 can be further simplified to:

$$R = 0.5 \times S_1 + 0.2389 \times S_2 + 0.132 \times S_5 + 0.07 \times S_{10} + 0.0318 \times S_{25} + 0.0135 \times S_{50} + 0.0138 \times S_{100} \tag{4.5}$$

4.3 Flow Velocity

Until recently, damage and risk calculations were performed only for flood events caused by the overflow of dikes, restricting the main cause of damage to water depth. However, overflow is not the only failure mechanism. Technical failures caused by dike/dune breaching may inflict damage to built-up areas that is much greater than that caused by overflow. In the vicinity of a breach, high flow velocities can even cause total collapse of buildings (Jonkman et al. 2008). Therefore, the potential for flow velocity damage needs to be incorporated into damage calculations based purely on depth. This additional damage cannot be greater than the difference between maximum damage and damage caused by water depth. Based on Vrisou Van Eck et al. (1999), new damage functions were developed combining levels of water depth with flow velocity (Verwaest et al. 2008).

In cases of breaching, flow velocity at a certain location is a function of three parameters: (i) distance to the breach, (ii) bottom shear, and (iii) the presence of obstacles in the inundated area (e.g., a road above ground level). The approach differs depending on whether a 1-D or 2-D hydraulic model is available.

In cases where hydrodynamic boundary conditions are known only from a 1-D model, no detailed information on depth or velocity in the inundated area is available. This limitation necessitates a conceptual approach (Kellens and Vanneuville 2007), which is schematically depicted in Fig. 4.5 and which represents a dike breach along a river. Around the breach, three concentric zones (A, B, C) are defined according to expected amounts of property damage. In Zone A, closest to

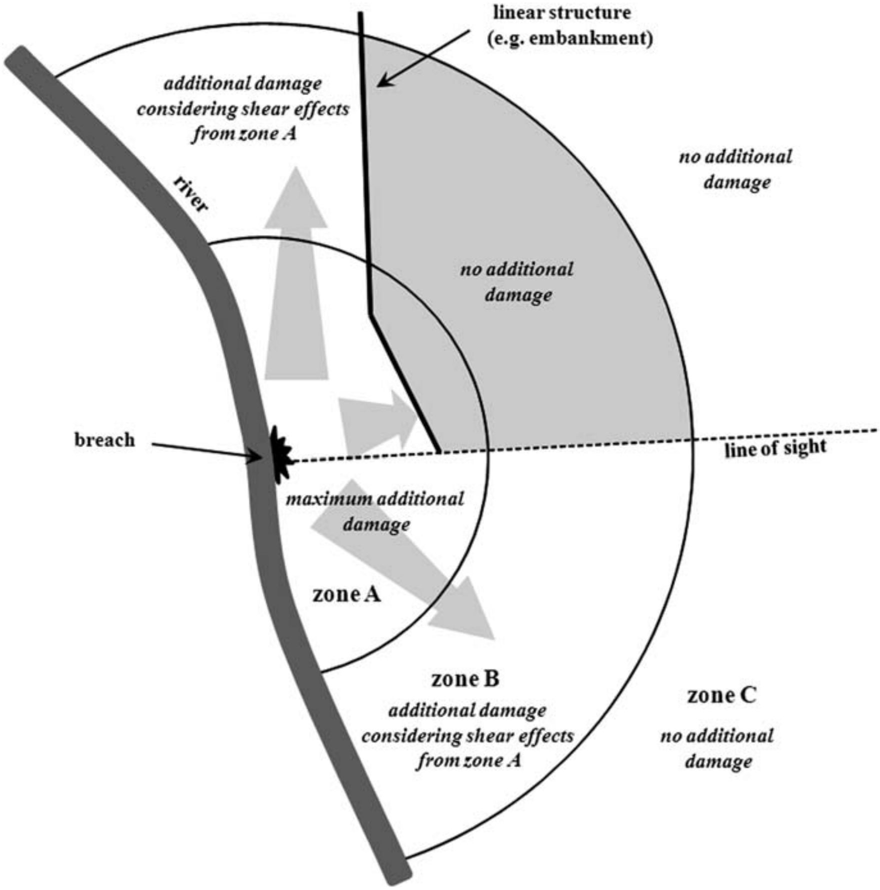

Fig. 4.5 Summary of the conceptual approach (Kellens and Vanneuville, 2007)

the breach, maximum additional loss is expected. Traveling away from the breach, flow velocities and damage decline because of shear and directional spreading of the water. The influence of shear depends on the land use in Zone A, as the water has to travel through this zone before it reaches Zone B; the influence of land use on flow resistance is based on Maijala (2001). The radii of Zones A and B are a function of the maximum discharge through the breach. The influence of barriers is also included; based on available vector data, possible obstructions for the traveling water are identified within the inundated area. Behind embankments no additional damage is expected provided there are no culverts or under-passes. The zone of influence of these barriers is determined by a line-of-sight analysis. Zone C sustains no additional damage.

In cases where water levels and velocity output are available from 2-D hydrodynamic models, Vrisou Van Eck et al. (1999) proposed combining flow velocity and water depth to determine maximum additional damage to construction due to breaching. Those authors considered a velocity of 3 m/s and a water depth of at least 0.5 m as necessary thresholds for buildings to collapse. For combinations of velocity and water depths lower than these values, continuous functions were constructed. The shape of the functions reflects the nature of the damage sustained: at low values for both parameters, losses are expected to be small. If either flow velocity or water depth increases, damage will increase dramatically until maximum additional losses occur.

4.4 Casualties

Besides material damage, floods cause human casualties due to the instability of people in rapidly flowing water and from building collapse (Jonkman et al. 2008). Although some have attempted to place a monetary value on human life (Card and Mooney 1977; Breyer and Felder 2005), a similar undertaking was not part of this study. Ramsbottom et al. (2003) and Jonkman and Vrijling (2008) denote the importance of water depth, rise velocity and flow velocity with regard to calculating loss of life caused by floods. The combination of great water depths and the rapid rise of water creates hazardous situations. People have limited time to reach higher floors or shelters and they may be trapped inside buildings. Consequently, the number of victims is calculated as the number of inhabitants multiplied by two proportionality factors, one for water depth and a second for rise velocity. Based on the findings of Jonkman et al. (2008), the model assumes 100% casualties if the water depth is higher than 6 m or if the rise velocity exceeds 3 m/h. For values lower than these thresholds, casualty functions were taken from Vrisou Van Eck et al. (1999).

An additional factor was added in the case of coastal inundations, where wave overtopping of coastal defense structures can create a substantial number of victims. Based on the work of Verhaeghe (2002) and Allsop (2005), an overtopping discharge of 0.095 l/m/s was set as the threshold value above which the maximum of casualties can be expected.

4.5 Implementation of the Methodology in a GIS

4.5.1 Early GIS-Model

The development of the risk-based methodology described above is insufficient, of itself, to perform risk analysis. The method needs to be translated into a useful model that executes all necessary steps in a pre-programmed chain of actions. Starting with land use maps and flood maps, all steps to create risk maps are separated into submodels based on a raster GIS approach. To determine whether to use raster or vector GIS, a preliminary study was performed (Vanneuville et al. 2003). While the tests did not produce large differences in precision nor accuracy, calculation times in raster GIS occur much more quickly than in vector GIS; 90% of the over 400 computations were more optimally performed in a raster-based GIS (Burrough and McDonnel 1998). One disadvantage of raster-based GIS is that the required storage capacities are much higher than for vector data; however, this is regarded as a minor issue (Eastman 2006).

The model was initially implemented in IDRISI® software (developed by Clark Labs, Clark University, Massachusetts) for raster GIS calculations. All operations were implemented using the software's model builder, which enables implementation of the different steps (as outlined above) within different submodels to reduce complexity. Unfortunately, the design of the software did not produce satisfactory results. As one example, it was necessary to perform time-consuming preprocessing of all necessary input layers and an intensive start-up procedure for each risk computation. The intensive start-up procedure made it difficult for other users in the organization who are unfamiliar with the methodology or IDRISI, to independently compute damage and risk maps.

Although the IDRISI model had possibilities (optimal computing capacities and built-in standard modules), its disadvantages led to the development of *LATIS*. *LATIS* is a GIS application that guides the user through each step of the different damage and risk calculations with a user-friendly interface.

4.5.2 Development of a Flood Risk Assessment Tool: LATIS

In 2007, Flanders Hydraulics Research, in cooperation with the Department of Geography at Ghent University developed a GIS tool named *LATIS* as a substitute for the model structure described above. One of the main prerequisites for the development of the tool was a user-friendly and easy accessible Graphical User Interface (GUI). Therefore, the GUI of *LATIS* (the "Client Application" in Fig. 4.6) is built in the C#.NET programming language. The interface of *LATIS* is a simple windows application, hiding the complexity of professional GIS software. The algorithms of the methodology are also implemented in C#.NET, but for the execution of the geospatial operations, *LATIS* still uses the optimal computing capacity and built-in standard modules (which perform the geospatial operations) of IDRISI. The .NET technology enables the use and execution (in the background)

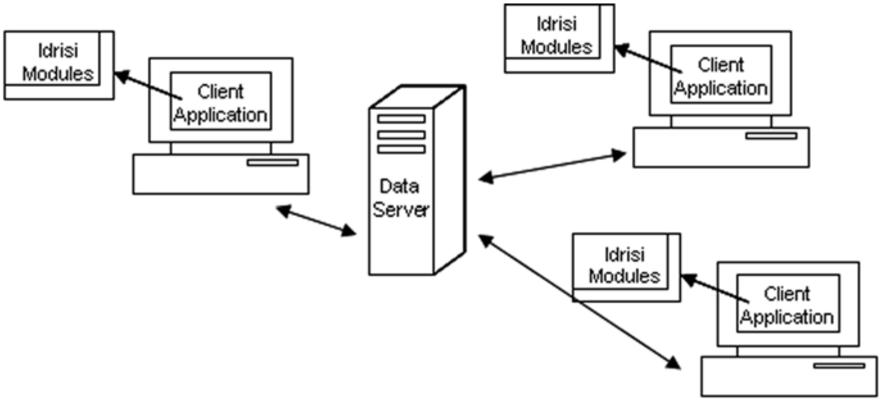

Fig. 4.6 Overview of the *LATIS* structure

of those IDRISI modules (Fig. 4.6, where the single-headed arrows represent the relationships between the client applications and the IDRISI modules), which are stand-alone executable files. The tool performs all necessary actions with the corresponding parameters in the background of the application so the user only has to input data that affect the risk calculations (i.e., the flood and land use maps and the socio-economic data).[4]

LATIS was also designed to address data management by developing a system that allows administrators to easily manage basic land use maps and socio-economic data. These maps and data are uniformly gathered for the extent of Flanders and are centrally managed on a data server. The manipulation of these base data is possible via the *LATIS* application of an administrator (shown in Fig. 4.6 by the arrows in the direction of the data server). When a user runs a damage and risk assessment, the application selects and extracts the necessary data (the standard is to select the most recent data) for the extent of a certain flooding scenario from the data server (shown in Fig. 4.6 by the arrows in the direction of the applications). Consequently, the application performs the preprocessing of land use and socio-economic data and the user only has to input the flood maps. The data management system also records what data is used in an assessment so a specific risk calculation can easily be repeated. Development of *LATIS* now allows damage and risk maps in Flanders to be calculated in an efficient, uniform, and reproducible manner.

4.6 LATIS in Action: Impact of Climate Change on Risk

The calculation of climate change scenarios in Flanders is one of the first projects for which the *LATIS* tool has been used. These climate change scenarios are based on regional climate models for different levels of CO_2 emissions. Based on potential

[4]*LATIS* is not an acronym – it is the Celtic goddess of water (and beer).

change in rainfall and evaporation rates, a high, mean and low scenario was defined for the summer and winter period in Flanders. In general, the potential for drought is expected to increase during the summer, while changes that may occur during the winter are highly uncertain (represented by a strong increase in flooding in the high scenario to a slight decrease in flooding in the low scenario).

The runs of the hydraulic model were executed based on the climate change scenarios and the available measurement series for water level, discharge and evaporation in order to derive catchment flood maps with different return periods. Both flood extent and water depth were used as the main factors influencing damage. Flood maps were used to recalculate damage and risk maps with the most recent socio-economic data available. These maps were used as references and compared with the flood risk maps produced under the climate change scenarios. For all four scenarios (current, low, mean and high), the flood risk is based on the same series of return periods as are used for flood map calculations (1, 50, 100 and 500 years).

A relatively small increase or decrease in water level can cause large differences in damage and risk. Vulnerable sites that are flooded once a century (on average) can be flooded more frequently, causing the risk to increase significantly. On the other hand, a large increase in water depth on agricultural land does not lead to a large increase in damage and risk because once crops are rotten, water depth is no longer important.

Economic damages are generally calculated for such features as housing, industry, and agricultural land. However, special attention is given to local features that are: (1) sensitive to extreme high damage values (e.g., power supply installations, museums), (2) important in case of an emergency (e.g., fire brigades, police stations) and (3) problematic due to evacuation reasons (e.g., hospitals, retirement homes).

Interpretation of the results of the damage and risk maps from the climate change scenarios is done (as for all flood risk assessments) in a relative manner. Because many generalizations are incorporated into the model, the risk values are not used as absolute stand-alone values – risk values of one scenario have to be compared with the risk values of other scenarios. Consequently, risk values between the scenarios are not compared on a pixel by pixel basis. Instead, the individual risk values in zones are grouped in order to evaluate scenarios. In the example of the Dender catchment (Table 4.1) the values are summarized in eight zones between two successive sluices and locks (Fig. 4.7).

As Table 4.1 indicates, the high scenario lead to a serious increase in monetary risk for the Dender catchment. In the master plan for this catchment – for which studies are already on-going – the location and dimensioning of the sluices will be evaluated and adapted. The proposed measures also have to be sustainable under conditions of climate change, so that the evaluated scenarios can be reused.

Figures 4.8 and 4.9 illustrate risk maps for part of the Dender catchment (the area covered by the rectangle in Fig. 4.7) representing the low (Fig. 4.8) and high (Fig. 4.9) climate change scenarios. These figures show a much larger spatial extent for risk in the high than the low scenario. For example, the factory at the south of the image is nearly 100% flooded in the high scenario compared to the low.

Table 4.1 Risk calculation for different climate change scenarios, Dender catchment (1000 euro/year)

Zone	Present	Low	Mean	High
1	806	148	445	1558
2	441	89	337	793
3	186	63	278	543
4	759	115	944	2426
5	257	126	320	1835
6	10	0	2	45
7	45	5086	5754	5933
8	720	276	374	423
Sum	3224	5902	8455	13,556

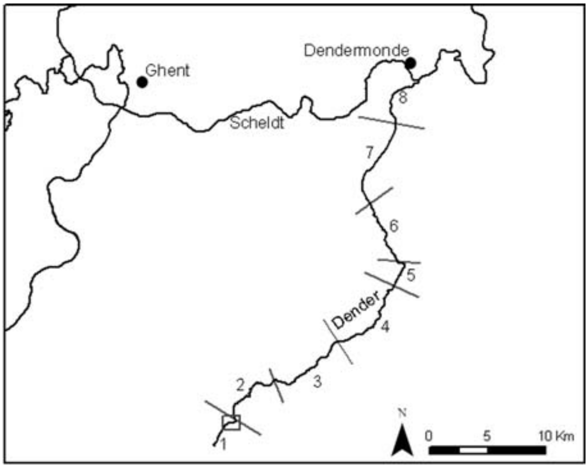

Fig. 4.7 Overview of the different zones in the Dender catchment (the *small rectangle* at the bottom of the figure indicates the location of the area shown in Figs. 4.8 and 4.9)
Source: Vectoriële versie van de "VHA-waterlopen & -zones", Vlaamse Milieumaatschappij – Afdeling Operationeel Waterbeheer (AGIV)

4.7 Conclusions and Further Developments

LATIS, a GIS application for assessing flood risk in Flanders, Belgium has been described, including an overview of the underlying risk methodology, which incorporates hydrologic and hydraulic models, land use information and socio-economic data. Presently, *LATIS* is being used as part of social cost-benefit analyses for estimating the effects of flood mitigation measures. These analyses are being performed in support of several riverine and coastal management plans, including studies on the widening and deepening of waterways, the construction of controlled flood zones, and proposed improvements in the coastal defense infrastructure. These plans not

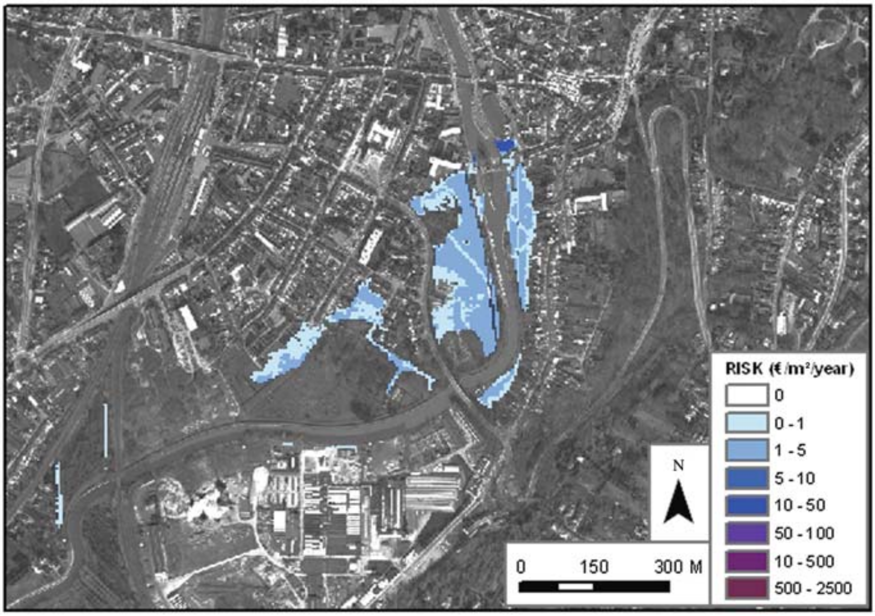

Fig. 4.8 Flood risk under the low climate change scenario in part of the Dender catchment Source of background map: Digitale versie van Orthofoto's, middenschalig, kleur, provincie Oost-Vlaanderen, AGIV en Provincie Oost-Vlaanderen, opname 2006 [GIS-Vlaanderen]

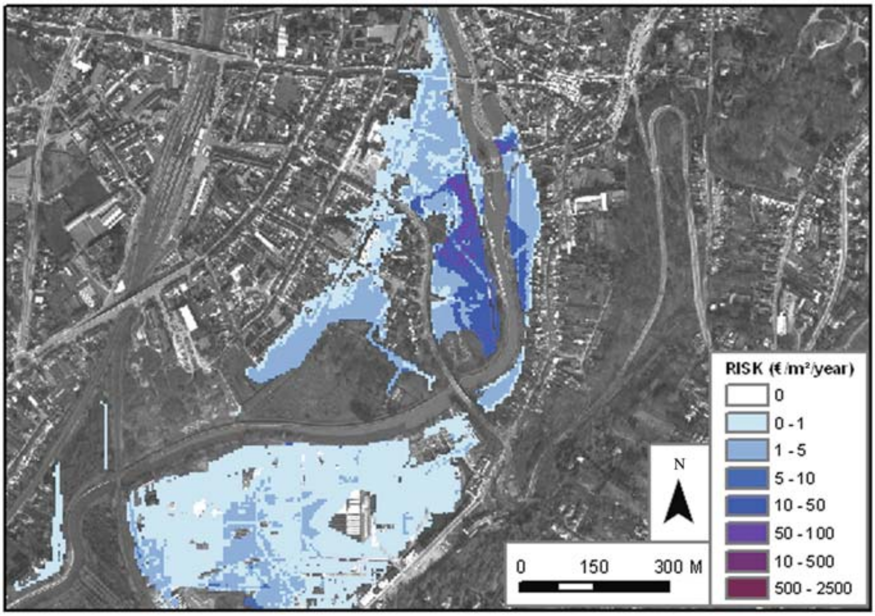

Fig. 4.9 Flood risk under the high climate change scenario in part of the Dender catchment Source of background map: Digitale versie van Orthofoto's, middenschalig, kleur, provincie Oost-Vlaanderen, AGIV en Provincie Oost-Vlaanderen, opname 2006 (GIS-Vlaanderen)

only seek to protect against current flood risk conditions but also to incorporate adjustments to deal with possible climate changes.

Currently, *LATIS* is limited to only four types of damage: monetary, internal, and direct/indirect. Future improvements to the methodology could include adding external and non-monetary damage to the model.

The model could be further improved with the use of more detailed base data. The main reason the current methodology uses aggregated data is pragmatic: data gathering is a time-consuming and costly job and processing time becomes longer with more detailed data. Therefore, the decision was made to work with generalized spatial data and to proceed gradually to more detailed data when more time and resources become available. This future work is important because estimating the number of people who could be afflicted directly impacts evacuation needs. Fortunately, although Flanders' flood plains are densely populated, it boasts a dense road network that is expected to support substantial evacuation numbers in the event of a calamity.

While flow velocity and the calculation of casualties due to floods were attempted, certain assumptions and simplifications were necessary for the present study. However, as these knowledge gaps are filled, more robust results could be produced. *LATIS* has proven its usefulness for calculating flood risk scenarios in Flanders. However, the real challenge lies in the near future, when European standards have to be met with respect to flood risk management. In 2007, the European Union released its European Flood Directive (2007/60/EC). In the next few years, all European member states have to comply with the demands described in that directive, most of which involve creating an inventory of objects in flood zones. Concurrent with that effort, potential flood damage and its likelihood will be evaluated, and necessary modifications made to improve the model. This on-going work will continue to strengthen *LATIS'* ability to function as an efficient data integration and data management system combined with a user friendly interface to improve flood risk management.

Acknowledgments The authors wish to acknowledge the financial support by the Flemish Government under contract WL16EB/06/07.

References

Ahola, T., Virrantaus, K., Krisp, J. M., Hunter, G. J. (2007). A spatio-temporal population model to support risk assessment and damage analysis for decision-making. *International Journal of Geographical Information Science*, 21(8), 935–953.

Allsop, N.W.H. (2005). D38: *Report on Hazard Analysis*. Report CLASH WP6, Coordinator HR Wallingford, 28p.

Breyer, F., Felder, S. (2005). *Mortality Risk and the Value of a Statistical Life: The Dead-Anyway Effect Revis(it)ed.* Geneva Risk and Insurance Review, 30(1), 41–55.

Burrough, P.A., McDonnel R.A. (1998). *Principles of Geographical Information Systems*, Oxford University Press, Oxford, p. 333.

Card W.I., Mooney G.H. (1977). What is the monetary value of a human life? *British Medical Journal*, 2, 1627–1629.

Cochrane, H.C. (2004). Indirect losses from natural disasters: measurement and myth. In: Okuyama, Y., Chang, S.E. (Eds.), *Modelling Spatial and Economic Impacts of Disasters*. Springer-Verlag, Berlin Heidelberg New York.

De Maeyer Ph., Vanneuville W., Maeghe K., Mostaert F. (2003). *Modélisation des effets de crue dans le bassin de la Dendre, basée sur une méthodologie de risqué* (Modelling the Effects of Flooding in the Dender Catchment based on a Risk Methodology), Le Geo Evenement, 4–6 march 2003, Paris, Actes des conférences sur Cd-rom, p. 7.

De Nocker, L., Broekx, S., Liekens, I. (2004). *Social Cost Benefit Analysis on Safety against Flooding in the River Scheldt Estuary – Conclusions on the Outlines*. VITO in cooperation with RA-IMDC, s.l., 92pp.

Eastman J.R. (2006). *Idrisi Andes, Guide to GIS and Image Processing*, Clark Labs – Clark University, Worchester, USA.

European Flood Directive. (2007). Directive 2007/60/EC of the European Parliament and of the Council, 23 October 2007. *Official Journal of the European Union*, L 288, 27–34.

Kellens, W., Vanneuville, W. (2007). *Damage and Risk Calculations, Report of Action 3b of the Interreg IIIB Project SAFECoast*, Ghent University and Flanders Hydraulics Research, Antwerp, Belgium, p. 41.

Jacobs, L., Worthley, R. (1999). A comparative study of risk appraisal: A new look at risk assessment in different countries. *Environmental Monitoring and Assessment*, 59(2), 225–247.

Jonkman, S. N., Vrijling, J. K. (2008). Loss of Life due to Floods. *Journal of Flood Risk Management*, 1(1), 43–56.

Jonkman, S.N., Vrijling, J.K., Vrouwenvelder, A.C.W.M. (2008). Methods for the estimation of loss of life due to floods: A literature review and a proposal for a new method. *Natural Hazards*, 46(3), 353–389.

Lekuthai, A., Vongvisessomjai, S. (2001). Intangible flood damage quantification. *Water Resources Management*, 15(5), 343–362.

Maijala M. (2001). *RESCDAM: Development of Rescue Actions Based on Dam-Break Flood Analysis.* Final Report June 1999–March 2001, p. 48.

Penning-Rowsell E., Johnson C., Tunstall S., Tapsell S., Morris J., Chatterton J., Coker A., Green C. (2003). *The Benefits of Flood and Coastal Defence: Techniques and Data for 2003*. Flood Hazard Research Centre, Middlesex University (book + CD-ROM with damage data).

Ramsbottom D., Floyd P., Penning-Rowsell E. (2003). *Flood Risks to People – Phase 1*. R&D Technical Report FD2317TR.

Simonovic, S.P., Carson, R.W. (2003). Flooding in the Red River Basin – Lessons from post flood activities. *Natural Hazards*, 28(2–3), 345–365.

Vaes, G., Willems P., Berlamont J. (2002). *Selectie en compositie van representatieve hydrogrammen voor riviermodellering.* Water, May 2002, p. 8.

Van de Sande, Corné (2001). *River Flood Damage Assessment using IKONOS Imagery*. In cooperation with the European Commission, Joint Research Centre, Space Applications Institute, EGEO Unit, Natural Hazards Project, Flood Damage and Flood Hazard assessment.

Van der Veen, A., Logtmeijer, C. (2005). Economic hotspots: Visualizing vulnerability to flooding. *Natural Hazards*, 36(1–2), 65–80.

Vanneuville W., De Maeyer Ph., Maeghe K., Mostaert F. (2003) Model the Effects of a Flood in the Dender Catchment, Based on a Risk Methodology. *Society of Cartography Bulletin*, 37(2), 59–64.

Vanneuville W., De Rouck K., Maeghe K., Deschamps M., De Maeyer Ph., Mostaert F. (2005). *Spatial Calculation of Flood Damage and Risk Ranking*, In: Conference Proceedings of Agile 2005, 8th Conference on Geographic Information Science, pp. 549–556.

Verhaeghe, H. (2002). *Toelaatbare Golfoverslag Over Zeeweringen: Literatuuroverzicht*. Universiteit Gent, vakgroep Civiele Techniek, Afdeling Weg- en Waterbouwkunde, intern rapport, p. 23.

Verwaest, T., Van Poucke, Ph., Reyns, J., Van der Biest, K., Vanderkimpen, P., Peeters, P., Kellens, W., Vanneuville, W (2008). *SAFECoast: Comparison Between Different Flood Risk Method-*

ologies: action 3B report, SAFECoast Interreg IIIb NorthSea project, Flanders Hydraulics Research, Belgium.

Vrisou Van Eck, N., Kok, M., Vrouwenvelder, A.C.W.M. (1999). *Standaardmethode Schade & Slachtoffers als gevolg van overstromingen – deel 2: Achtergronden*, HKV-Lijn in Water en TNO Bouw in opdracht van RWS-DWW.

Yates, S. (1992). Lay attributions about distress after a natural disaster. *Personality and Social Psychology Bulletin*, 18(2), 217–222.